Available online at www.sciencedirect.com
ScienceDirect
Planetary and Space Science 54 (2006) 1073–1085
Planetary and Space Science
www.elsevier.com/locate/pss

VUV photochemistry of small biomolecules

Martin Schwell[a,*], Hans-Werner Jochims[b], Helmut Baumgärtel[b], François Dulieu[c], Sydney Leach[c]

[a]*Laboratoire Interuniversitaire des Systèmes Atmosphériques (LISA), Faculté des Sciences, CNRS-UMR 7583, Université Paris 7 & 12, 61 Avenue du Général de Gaulle, 94010 Créteil, France*
[b]*Institut für Physikalische und Theoretische Chemie der Freien Universität Berlin, Takustr. 3, 14195 Berlin, Germany*
[c]*Laboratoire d'Etude du Rayonnement et de la Matière en Astrophysique (LERMA), CNRS-UMR 8112, Observatoire de Paris-Meudon, 5 place Jules-Janssen, 92195 Meudon, France*

Accepted 10 April 2006
Available online 13 July 2006

Abstract

We review our recent results on the vacuum ultraviolet (VUV) photochemistry of small biomolecules. The experimental techniques used, mass spectrometry and photofragment fluorescence spectroscopy, are described. Emphasis is laid on our mass spectrometric results obtained for five nucleic acid bases and five amino acids. Ionisation and appearance energies are determined from photoionisation mass spectrometry, many for the first time. From this, fragmentation pathways following 6–22 eV photoexciation are derived. The adiabatic ionisation energies of the biomolecules studied lie between 8.2 eV (adenine) and 9.6 eV (α-amino-isobutyric acid). We show that the nucleic acid monocations, and chemically related molecular cations, do not fragment even when formed with large internal energies (E_{int}) ranging from 1.80 to 5.35 eV. In contrast, amino acid monocations are unstable and rapid fragmentation occurs via rupture of the C–C(OOH) bond, except for β-alanine, where rupture of the bond between the α-C and β-C is the lowest lying ionic dissociation channel. The VUV photochemistry of the prebiotic species formic acid, acetic acid and methylformate, studied in more detail previously by several techniques, including fluorescence spectroscopy, is also reviewed. Astrophysical implications of our work are discussed in the conclusion.

Keywords: VUV-astrochemistry; Nucleic acid bases; Amino acids; Photoionisation mass spectrometry; Photofragment fluorescence spectroscopy

1. Introduction

Small biomolecules, like nucleic acid bases (NABs) and amino acids (AAs) or chemically related molecules, have so far not been identified in the interstellar medium (ISM) or in other extraterrestrial media like cometary or planetary atmospheres, except possibly for glycine which has been reported from radioastronomy searches in the hot molecular cores Sgr B2(N-LMH), Orion KL, and W51 e1/e2. (Kuan et al., 2003a). Upper limits of abundance have been established for pyrimidine (Kuan et al., 2003b) and imidazole (Irvine et al., 1981). Pyrimidines and purines, the molecular skeletons of biologically important NABs, have been reported in the data obtained with the PUMA dust impact mass spectrometer during the flyby of comet Halley by the Soviet spacecraft VEGA 1 (Kissel and Krueger, 1987), however no molecular speciation could be inferred from these spectacular in-situ measurements. The difficulty in identifying these molecules by spectroscopic remote sensing techniques is probably due to their small abundances as well as current instrumental limitations. Furthermore, microwave and optical transitions in large molecules are in general more difficult to detect because the intensity of each band is reduced by a large partition function. The biomolecules could also be condensed on interstellar grains or icy comets. Their specific spectral features would be even more difficult to detect under these conditions since they would be modified by the surrounding matrix.

On the other hand, purine based NABs, as well as certain hydroxyl-pyrimidines, have been reported to have been found in the formic acid extract of the carbonaceous meteorites Murchison, Murray and Orgueil

*Corresponding author. Tel.: +33 1 4517 1521; fax: +33 1 4517 1564.
E-mail address: schwell@lisa.univ-paris12.fr (M. Schwell).

0032-0633/$ - see front matter © 2006 Elsevier Ltd. All rights reserved.
doi:10.1016/j.pss.2006.05.017

(Hayatsu et al., 1975; Stocks and Schwartz, 1981; Hua et al., 1986). We note however, that no additional publications appeared in the last 20 years to confirm these results, although several research teams tried intensively to identify these important molecules using ultra-modern analytical methods. Hence, at present one cannot conclude on an extraterrestrial presence of NABs.

AAs are also found in meteorites and micrometeorites (see chapters by J.L Cronin and M. Maurette in Brack, 1998). In these objects they could be embedded in polymer material. The chemical structure of this refractory polymer material is hitherto unknown (cf. Cronin, 1976a, b; Cronin and Pizzarello, 1983; Muñoz Caro et al., 2002). The abundance of AAs in meteoritic material strongly suggests their extraterrestrial presence.

As to the formation of small biomolecules in an astrophysical context, this is a vast subject that can not be treated in this article (for further reading see the books edited by Brack, 1998 and Chela-Flores et al., 2001). To give a glimpse here, earlier laboratory work has suggested that, for example, purines and pyrimidines may be formed in the ISM starting from hydrogen cyanide or cyanoacetylene (Basile et al., 1984), or even more simple gases like NH_3, N_2, CO_2 and H_2O (Lavrentiev et al., 1984). Pyrolysis-GC-MS has been applied to analyse HCN-polymers which are thought to be among the organic macromolecules most readily formed within the solar system, for example within planetary and cometary atmospheres. These experiments led to the identification of the purine based NABs adenine and xanthine (as methylated derivatives), as well as other nitrogen heterocycles (Minard et al., 1998). Recently, Muñoz Caro and co-workers (2002) have shown that the hydrochloric acid extract of the so-called ''yellow-stuff'', formed under UV irradiation of simulated interstellar ices in the laboratory, contains numerous AAs.

Exploring the VUV photochemistry of these important biomolecules is of considerable interest from an exobiological point of view, because of the possible delivery of these molecules from space to the early Earth, and the role that they could have played in the origin and development of life on earth, and possibly on other planets or satellites (Brack, 1998; Maurel and Décout, 1999; Sowerby and Heckel 1998; Sowerby et al., 2001). Furthermore, in the VUV spectral domain ($E_{photon} \approx 6-20$ eV; $\lambda \approx 62-200$ nm), the photoabsorption cross section of these molecules is even higher as compared to the mid-UV ($\lambda = 200$–400 nm, $E < 6$ eV) (see for example the pioneering monograph of Robin, 1974). In particular, all absorb strongly at $E = 10.2$ eV, where the intense Lyman-α stellar emission is located. Most of the small biomolecules studied have first ionisation energies (IE) below this energy, making ionisation phenomena an important issue to study. Additionally, we note that, in connection with the possible earthbound delivery of biotic molecules from space, the VUV luminosity of the early sun, during the Hadean period of considerable bombardment of the Earth from space was about two orders of magnitude higher than it is today, although the total luminosity was less (Chyba and Sagan, 1992).

Besides valence transitions, resonant excitation to Rydberg orbitals can also take place in the VUV spectral domain. These sharp electronic transitions converge to the 1st or higher ionisation energies. Beyond the first IE they are usually superimposed on a broad ionisation continuum. Their assignment can be achieved using the modified hydrogen series formula $E_n = \mathrm{IE} - [R/(n-\delta)^2]$ where the value $E_n - \mathrm{IE}$ gives the energetic distance for the Rydberg orbital to the corresponding IE (Robin, 1974). The principal quantum number n and the Rydberg constant R ($R = 13.605$ eV) have the same significance as in the hydrogen atom orbital structure. For the hydrogen atom δ equals 0, and the first member of the series ($n = 2$) is found at $E \approx 10.2$ eV corresponding to about 3/4 of the ionisation energy. The value $(3/4) \times \mathrm{IE}$ can be used to find the first member of a Rydberg series. For molecules, the quantum defect value δ is introduced which depends on the electronic structure of the positively charged molecular core (corresponding to its deviation from the ideal ''point charge'' H^+). The vibrational structure of Rydberg transitions in molecules can be identified with the aid of photoelectron spectra: Since the electrons populating the Rydberg orbitals are far from the molecular core, the vibrational frequencies of the latter are close to those of the corresponding cation.

Absorption of VUV photons can induce many important photo-processes, such as direct ionisation, autoionisation (resonant excitation of an excited state beyond the IE with subsequent coupling to the ionisation continuum releasing the ionised species), dissociative photoionisation, fluorescence of photofragments formed in excited states, as well as ion pair formation which can occur below and beyond the first IE. For a detailed review of these processes see Berry and Leach (1981). They can be explored by numerous experimental techniques, such as photoabsorption spectroscopy, photoion mass spectrometry (PIMS), photofragment fluorescence spectroscopy (PFS), photoelectron spectroscopy, to name only a few. In Section 2, we present in more detail two techniques used intensively by our group: PIMS and PFS in connection with synchrotron radiation (SR) as the photon excitation source. In Sections 3.1 and 3.2 of this article we highlight our work on the VUV photochemistry of NABs and AAs, published in more detail very recently (Jochims et al., 2004, 2005) and discuss their photostability. Section 3.3 will deal with more simple, ''prebiotic'' species studied also by our group.

To complete this introduction, we mention that also in the mid-UV, of course (neutral) photochemistry may occur, however photoabsorption cross sections are lower (Callis, 1983). This spectral domain is more accessible to experiments with pulsed lasers where the time-scales of photophysical processes following UV excitation can be studied. For example, the gas phase mid-UV photochemistry of purine NABs has been explored recently by resonant two-photon ionisation spectroscopy (Nir et al., 2001;

Lührs et al., 2001; Plützer et al., 2001; Plützer and Kleinermanns, 2002). Interestingly, the most prominent feature of the NABs mid-UV photochemistry in the gas phase is that internal conversion upon excitation in the 280–300 nm range, where the lowest lying excited electronic states are located, occurs very fast, on the pico-second time-scale. The purine nucleobases are therefore protected from mid-UV induced fragmentation. It has been argued that this could be the reason why evolution has arrived at this particular building block to store genetic information (Broo, 1998).

Recently, the photostability of AAs and NABs has also been studied in argon matrices at 12 K, irradiated by a microwave excited low pressure hydrogen lamp (Ehrenfreund et al., 2001; Peeters et al., 2003). This kind of lamp delivers a multiline emission spectrum with photons of wavelengths between 165 and 135 nm (7.5 eV < E < 9.2 eV). These experiments indicate that NABs and AAs are degraded photochemically at these wavelengths in an argon matrix (at 12 K). However, no wavelength dependent data nor quantum yields of photodissociation are obtained from these experiments. The derived "UV destruction cross sections", averaged over all wavelengths emitted by the hydrogen lamp, can be regarded as the product of the absorption cross section σ_{abs} and the photodissociation cross section σ_{diss} in the mixed solid state. They should be strongly dependent on (a) the mixing ratio inside the solid phase and (b) on the chemical nature of the solid phase in which they are embedded. Application of these UV destruction cross-sections to other solid phases than argon, for example to interstellar grains, or the gas phase should be handled with caution.

We finally indicate that gas phase measurements of NABs and AAs are also of significance for biology concerning the comprehension and determination of properties of these basic units when free from interactions.

2. Experimental methods to explore VUV photochemistry

Fig. 1 gives an overview of the different experimental set-ups used in our experiments. Different kind of experiments can be connected to the monochromator at the respective beamline. They will be described in the following.

2.1. Synchrotron radiation as a light source

SR is a very bright, broadband, polarised and pulsed source of light. Brightness is defined as photon flux per unit area and per unit solid angle. It is a more important quantity than light flux alone, particularly in applications where monochromators are used (so called "throughput-limited applications"). SR, linked to an appropriate monochromator, is an extremely important light source for the exploration of VUV photophysics and photochemistry. Its advantage, for example as compared to lasers, is mainly due to the spectral broadness of the available photons and the resulting ease of wavelength tunability in the VUV. The energetics of fragmentation channels can therefore easily be explored.

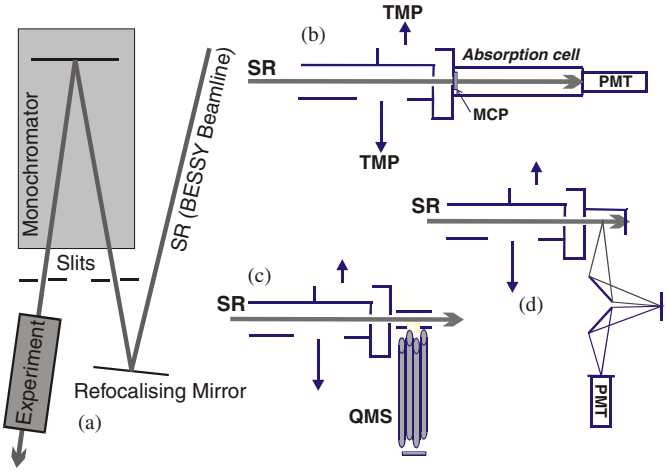

Fig. 1. Schematic schemes of the experimental set-ups used. (a) General setup. (b) VUV photoabsorption measurements. (c) Photoion mass spectrometry. (d) Photofragment fluorescence spectroscopy. SR = synchrotron radiation, TMP = turbomolecular pump, MCP = microchannelplates, PMT = photomultiplier tube, QMS = quadrupole mass spectrometer.

In electron storage rings designed as SR sources, there are three possible sources of radiation: dipoles (bending magnets), wigglers which act like a series of bending magnets with alternating polarities, and undulators which consist also in a sequence of multiperiod alternating magnet systems but in which the beam deflections are small resulting in a coherent interference of the emitted light and consequently in very high flux. In typical storage rings, several bunches of up to 10^{12} electrons circulate in an ultra-high vacuum, guided by the magnet fields of the dipole magnets. The most important characteristic for accelerators/rings designed especially for SR sources is that they have magnetic focusing systems which are able to concentrate the electrons into bunches of very small cross-section and where the electron transverse velocities are small (otherwise electrons are lost rapidly and the ring current would decrease fast, with undesired consequences on data acquisition times). The combination of high intensity with small apertures and small source dimensions results in a very high brightness. For further reading on SR see S.L. Hulbert and G.P. Williams in Samson and Ederer (2000).

In our experiments, SR was mainly obtained from the electron storage rings BESSY I and II, at Berlin. Our experiments are continuous in nature, thus do not take advantage of the pulsed structure of the light. A modified 1.5 m McPherson normal incidence monochromator ("NIM"), at the end of a dipole magnet beamline, has been mainly used in the studies presented here. Very recently, also 3 and 10 m focal length monochromators have been employed for completing measurements. The spectral bandwidth can be as low as 0.05 Å or less at the

currently used beamline at BESSY II (1200 lines/mm grating mounted on a 10 m focal length monochromator at the U125/2 undulator beamline). Generally, high resolution measurements can be necessary (a) if the data are to be incorporated into photochemical models since the solar Lyman-α emission is also very narrow (0.1 Å), but also (b) for exploring the temperature dependence of photoabsorption bands which is very important in space and planetary sciences.

2.2. Photoabsorption cross section measurements in the VUV spectral region

Absolute photoabsorption cross sections of many of the molecules studied by our group, especially NABs and AAs, have so far only been reported from measurements of films, because of the low volatility of these molecules. Their thermal fragility makes them difficult to measure at high temperatures. Using films, the optical reflectance is investigated and the absorption coefficient can be extracted (see for example Arakawa et al., 1986). Another possibility to obtain the optical constants of molecules of very low volatility is to record their electron energy loss spectra (EELS, see for example Isaacson, 1972). This technique also uses thin films as the substrate for measurements.

An inherent problem of the earlier gas phase measurements of the more volatile species, such as formic acid or acetic acid, is that the measurements of absolute absorption cross sections were often limited to energies below approximately 11 eV, corresponding to the cut off of the window material used in the absorption cell (see for example Robin, 1974; Suto et al., 1988). In our photoabsorption measurements we use a microchannel plate to delimit the optical path length in our absorption cell. This material transmits a sufficient portion of light to perform measurements and at the same time is an excellent barrier for gas phase molecules. We can therefore determine absolute absorption cross sections using the Beer–Lambert-Law beyond the above mentioned energy limit, which is of interest in an astrophysical context.

2.3. Photoionisation mass spectrometry

Since photoionisation and dissociative photoionisation are very important processes in the VUV, mass spectrometry is an excellent tool to get more insight into VUV photochemistry. In our experiments, monochromatised SR is focused into a differentially pumped gas cell which can be heated up to 400 °C in order to vaporise compounds in the liquid or solid state. They are placed 1–2 cm below the position of the incident VUV radiation within the ion extraction zone. The experimental set-up is described in more detail by Schwell et al. (2000). When thermally labile, biological compounds are investigated, the temperature has to be kept as low as possible. For example, experiments on NABs were typically performed at about 100 °C. This temperature was sufficient to provide an adequate stream of target molecules towards the ion source. When some thermally induced dissociation did occur this was easily identified in the observed mass spectra. For example, in the case of AAs, the appearance of an enhanced CO_2 mass peak ($m/z = 44$), enabled us to modify experimental parameters in order to achieve suitable experimental conditions of minimal thermal dissociation and satisfying signal intensity.

The photoion yield curves of parent and fragment ions (see Fig. 3 for example) were measured using a quadrupole mass spectrometer (Leybold Q200) which records the intensity of a given mass as a function of the incident photon energy. Measuring intervals are typical about 10 meV. The yield curves of the ions are normalised to the incident photon flux which is measured by detecting the fluorescence of a sodium salicylate coated window. Photon flux variations are due to the grating transmission function of the primary monochromator and descending storage ring current. The spectral bandwidth of the incident monochromatic radiation applied during PIMS measurements was typically 2 Å corresponding to an energy resolution of about 25 meV at a wavelength of 1000 Å. Ionisation energy determinations are carried out with a MgF_2 filter (100% cut-off effective at 11 eV) in order to suppress high energy stray light and second-order radiation which is an inherent problem of experiments with monochromatised SR. Ion appearance energies were determined mainly with the aid of semi-log plots of the ion yield curves. For many of the biological molecules under study here, we report adiabatic ionisation energies and fragment appearance energies (AE) that were previously unknown. Also, the limited data previously available, mainly from electron impact measurements, suffer often from unsatisfactory precision and poor detection sensitivity resulting in too high IE and AE values and large errors. More precise AE data for these compounds, measured with photon impact, are therefore important in order to explore the energetics of their VUV degradation pathways. In particular, this information permits assessment, on thermochemical grounds, of possible ionic and neutral products, as well as enabling one to choose between alternative dissociation channels.

The measured fragment AEs are *effective* thermochemical values. They are a function of instrumental detection sensitivity and also reflect effects of thermal energy since any activation barrier of a particular fragmentation process (1) could lead to depositing internal or kinetic excess energy in the fragments. Measurement of AEs are subject to this so-called "kinetic shift". In this respect, our measured AEs represent upper limit values. Using Eq. (2), the AEs are used to calculate *apparent* enthalpies of formations of the respective fragment ion m_1^+ ("*app*-$\Delta_f H^\circ$ (m_1^+)") which can be formed by different possible fragmentation pathways. Here, also different and/or several neutral fragments m_i, including isomers, have to be considered.

$$M + h\nu \rightarrow M^+ + e^- \rightarrow m_1^+ + xm_i, \quad (1)$$

$$app - \Delta_f H^{\circ}_{\mathrm{gas}}(m_1^+) = \mathrm{AE} + \Delta_f H^{\circ}_{\mathrm{gas}}(M) - \sum_{i=1}^{x}[\Delta_f H^{\circ}_{\mathrm{gas}}(m_i)]. \quad (2)$$

The measured apparent $\Delta_f H^{\circ}{}_{gas}$ (m_1^+) values are then compared to tabulated standard thermochemical enthalpies of formation $\Delta_f H^{\circ}(m_1^+)$, if available, thus permitting assignment of particular fragmentation channels (see for example the scheme presented in Fig. 4 which has been derived from our measurements as discussed in Jochims et al., 2005). If literature $\Delta_f H^{\circ}$ (m_1^+) values are not available, the measured app-$\Delta_f H^{\circ}$ values represent new values to be used in the future for m_1^+. We also hope to incite theoretical work with our measurements, on the thermochemistry of these fragments (neutral and cationic) in order to clarify further the fragmentation pathways.

2.4. Photofragment fluorescence spectroscopy

For fluorescence measurements, the SR light beam is focused into an open brass cell, differentially pumped, containing the vapour to be studied at a typical pressure of about 10^{-3} mbar. The induced fluorescence, in general produced by photo-excited fragments, passes through a quartz window and is dispersed using a 20 cm focal length monochromator (Jobin-Yvon H20, dispersion 4 nm/mm). In our experiments we generally observe the emitted fluorescence in the 250–550 nm spectral region, with a resolution depending on the choice of the exit slit (0.5, 1, or 2 mm). The spectral response function used for deconvolution of the observed spectra, has been determined by recording the emission of a tungsten halogen lamp. When recording the fluorescence excitation (FEX) spectra, the H20 secondary monochromator is fixed at a desired wavelength (for example at $\lambda = 310$ nm corresponding to the OH ($A^2\Sigma^+ - X^2\Pi$) transition) with a large exit slit. The primary monochromator is then tuned in steps of typically around 30 meV. The observed FEX spectrum reveals, in conjunction with the photoabsorption spectrum, the electronic states of the parent molecule producing the emitting photofragment (see for example Fig. 6b). After appropriate calibration of the observed fluorescence intensity, state selective quantum yields of a particular fragmentation channel can be derived. In contrast to mass spectrometry, fluorescence spectroscopy enables us to explore fragmentation processes below the ionisation limit.

3. Selected results

In this section we present selected results obtained recently. A detailed discussion of these results can be found in the cited references. Fig. 2 gives an overview of the molecules studied by our group in recent years.

3.1. Ionisation and dissociative ionisation of nucleic acid bases

NABs have been studied by PIMS (Jochims et al., 2005; Schwell et al., 2006). Table 1 summarises our results on

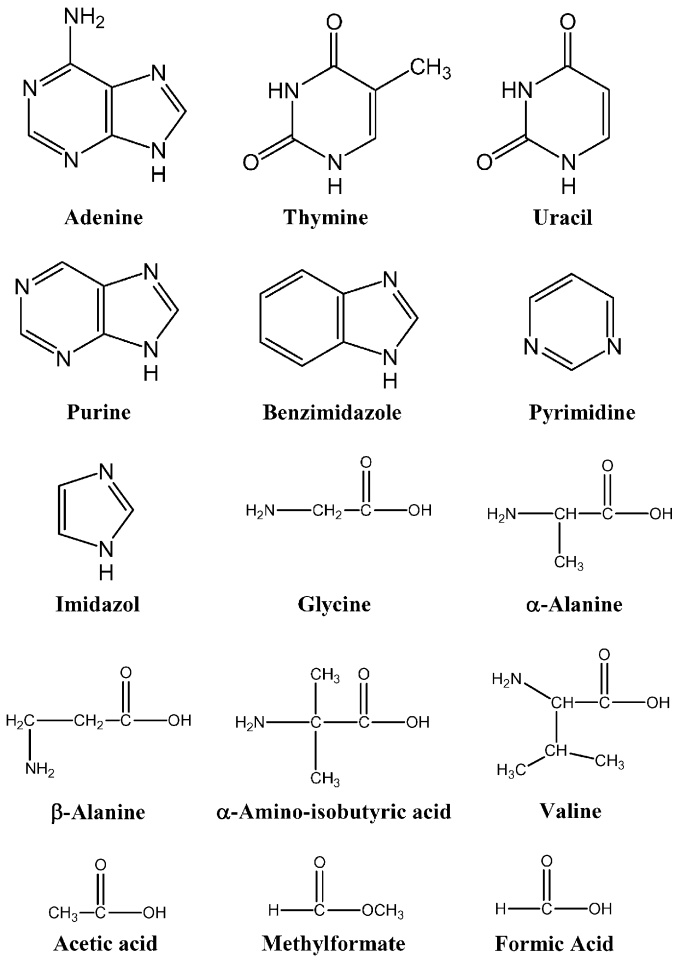

Fig. 2. Biomolecules and prebiotic species investigated in recent years by our group.

NABs and also on AAs. We show measurements of the first ionisation energy together with appearance energies of the lowest lying ionic dissociation channel. The third column gives the difference between these two values indicating the internal energy E_{int} necessary to photodissociate the respective molecule at a particular rate. It has been shown in earlier work (Jochims et al., 1994), where the same experimental equipment was used, that our observed AEs correspond to a photodissociation rate of about $k_{\mathrm{diss}} = 10^4\,\mathrm{s}^{-1}$ at the energy of the ion onset. This estimation is based on RRK model calculations (RRK = Rice, Ramsperger, Kassel theory) of the photodissociation rate of polycyclic aromatic hydrocarbons (PAHs), in particular their H-loss reactions which are the energetically lowest lying VUV photodissociation channels in PAHs (for details see Jochims et al., 1994). It is valid for other molecules and other fragmentation reactions too, since k_{diss} at the observed threshold of ion formation is an experiment-specific quantity.

The NABs studied have E_{int} values ranging from 1.80 eV (uracil) to 3.36 eV (adenine). For the non-biological base benzimidazole E_{int} equals 5.35 eV. These values are fairly large but slightly lower than in PAHs where values from

Table 1
First ionisation energy (IE, adiabatic value), lowest appearance energy (first fragment AE) and E_{int} as measured by photoionisation mass spectrometry (the given errors represent the experimental uncertainty of the ion onset as read from the respective photoion yield curves)

	First IE (eV)	First AE (eV)	E_{int} (eV)	Dissociation channel
Adenine	8.20±0.03	11.56±0.05	3.36±0.08	HCN loss
Purine	9.35±0.05	12.6±0.05	3.25±0.1	HCN loss
Benzimidazole	8.22±0.05	13.57±0.1	5.35±0.15	HCN loss
Thymine	8.82±0.03	10.70±0.05	1.88±0.08	HNCO loss
Uracil	9.15±0.03	10.95±0.05	1.80±0.08	HNCO loss
Pyrimidine	9.05±0.05	12.27±0.05	3.22±0.1	HCN loss
Imidazole	8.66±0.03	11.41±0.05	2.75±0.08	HCN loss[a]
Glycine	9.02±0.02	9.38±0.05	0.36±0.07	$NH_2CH_2^+ + COOH$
α-Alanine	8.75±0.05	9.05±0.1	0.3±0.15	$NH_2CH_3CH^+ + COOH$
β-Alanine	8.8±0.1	9.3±0.1	0.5±0.2	$NH_2CH_2^+ + CH_2COOH$
α-Amino-isobutyric acid	9.6±0.2	9.1±0.1[b]	(0)	$NH_2C(CH_3)_2^+ + COOH^-$
Valine	8.9	—	—	$NH_2(CH_3)_2(CH)_2^{+c} + COOH$

[a]Two other dissociation channels (H loss and HCN + CH loss) have similar appearance energies (see Schwell et al., 2006).
[b]Ion pair formation below first IE.
[c]Most intense cation at $E = 20$ eV.

4.62 (benzene) to 12.05 (coronene) were observed (Jochims et al., 1994). Another difference is that the lowest lying dissociation reaction in PAHs is H-loss from the parent cation whereas in NABs these are the HCN and HNCO loss reactions although they both require rupture of at least two bonds. The reason for this is most certainly the thermodynamically stable HCN molecule ($\Delta_f H^\circ = 1.401$ eV (Chase, 1998)). For the molecules presented in this study, below 20 eV photon energy the H loss reaction is either not observed or the corresponding $(M–H)^+$ ion is very weak, except for imidazole (Mol. mass = 68.08 a.m.u.) where AE ($m/z = 67$) is observed to be 12.05±0.03 (Schwell et al., 2006).

As an example of our PIMS measurements we show photoion yield curves of the adenine parent cation (Mol. mass = 135.13 a.m.u.) and its most important fragment ions (Fig. 3). We determined the adiabatic ionisation energy to be 8.82±0.03 eV. In Fig. 4, we show the adenine fragmentation scheme as deduced from our measurements and earlier measurements obtained with electron impact (EI) ionisation (cf. also our detailed discussion and references cited in Jochims et al., 2005). Chemical structures of important ions are also proposed in Fig. 4. However, these structures have to be confirmed by theoretical work to be performed in the future.

The principal fragmentation pathways involve four successive losses of neutral HCN molecules as indicated in Fig. 4 together with the corresponding appearance energies AE measured by PIMS. The initial HCN fragmentation, involving atoms 1 and 2 (see numbering used in Fig. 4), requires two bond ruptures. It is more energy consuming than the succeeding HCN losses which each probably require only one bond rupture in the precursor fragment ion and/or it corresponds to successively smaller total reorganisation energy. The loss mechanisms could be quite complex and may involve loss of HNC as well as HCN. The fate of the primary fragment

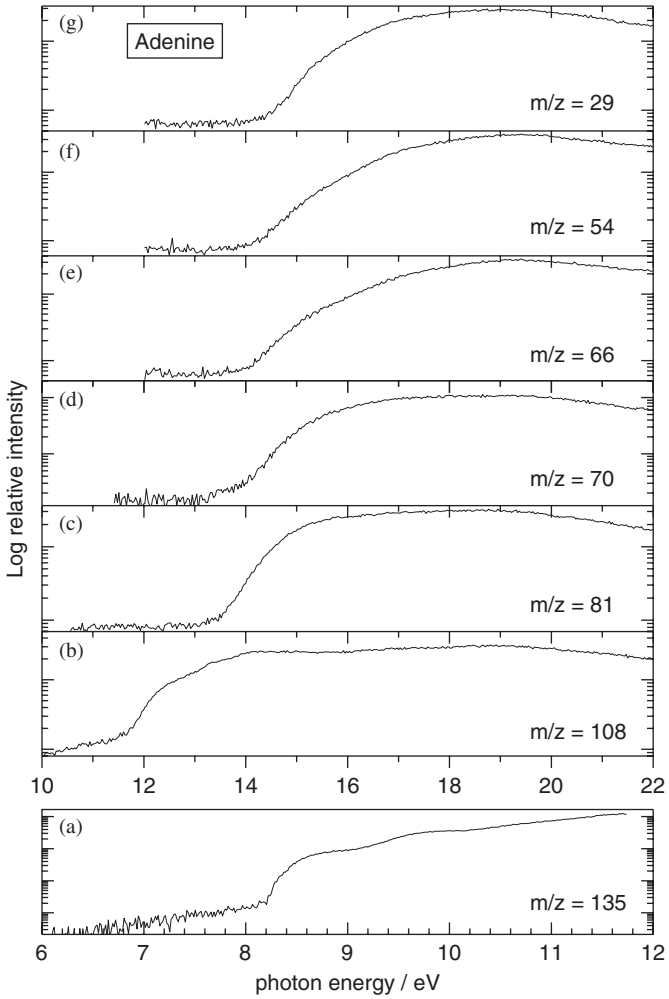

Fig. 3. Selected photoion yield curves of adenine (we note that in Fig. 2 of the original publication (Jochims et al., 2005) an error has occurred: There, $m/z = 65$ is actually $m/z = 66$ and 53 is actually $m/z = 54$. This has been corrected here).

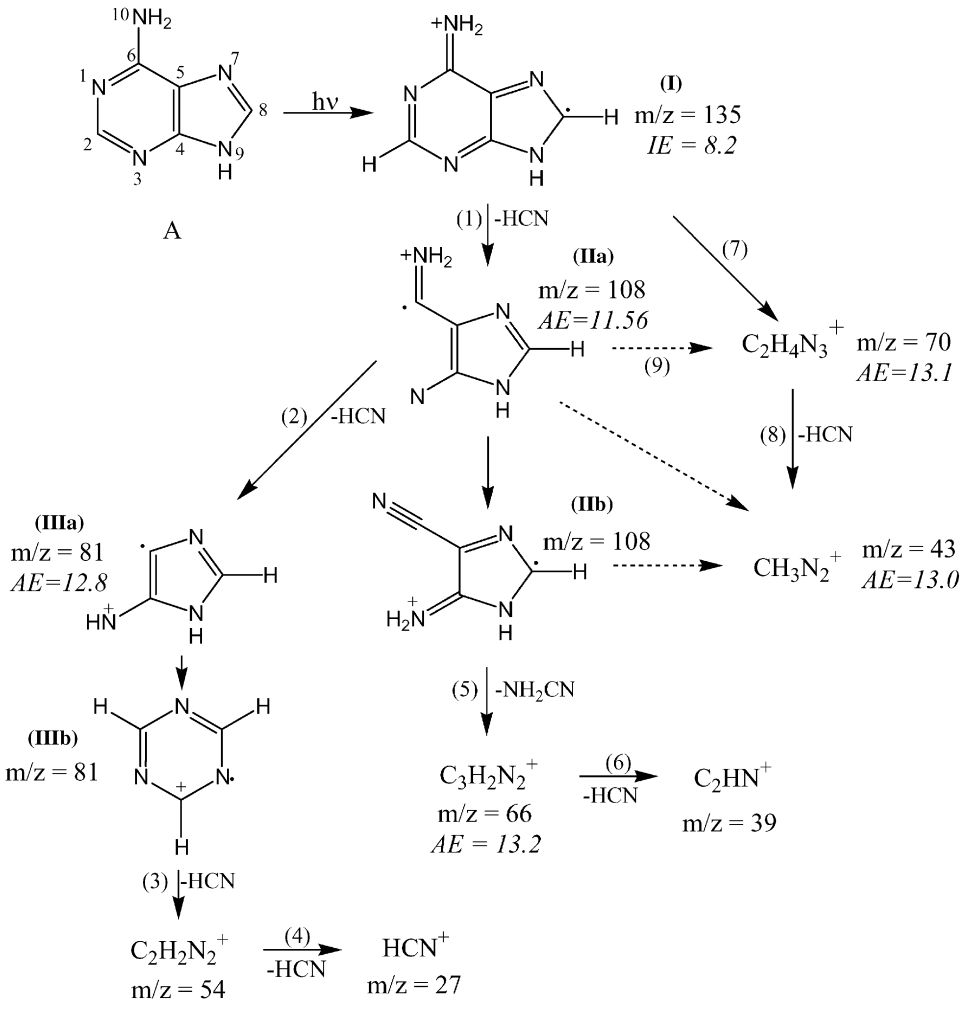

Fig. 4. Scheme of the VUV induced fragmentation of adenine. The measured appearance energies (IE and AEs) for each ion are also indicated (in eV, for experimental errors refer to Table 1).

IIa ($m/z = 108$) can be either loss of C_2N to give the ion $m/z = 70$ or isomerisation to species IIb which is probably thermodynamically more stable. This species subsequently loses NH_2CN to give the important ion $m/z = 66$ which can in turn lose a neutral HCN unit. The intense ion $m/z = 43$ ($CH_3N_2^+$) can be formed by several pathways as indicated in Fig. 4. A similar picture comes out from our recent measurements on purine and benzimidazole (Schwell et al., 2006): In purine (Mol. mass = 120.11 a.m.u.), successive loss of two HCN molecules is also the predominant fragmentation pathway at low energies ($E < 13.6$ eV). The respective appearance energies are 12.6 ± 0.05 and 13.24 ± 0.1 eV. The parent cation of the non-biological base benzimidazole (Mol. mass = 118.14 a.m.u.) shows a remarkable stability domain, from 8.22 ± 0.05 to 13.57 ± 0.1 eV ($E_{int} = 5.35 \pm 0.15$ eV, see Table 1).

In thymine, the dominant fragmentation reaction is loss of HNCO (Isocyanic acid, see Table 1) by Retro–Diels–Alder reaction from the parent cation to give the $m/z = 83$ ion (AE = 10.7 eV). This ion, which may have a cyclic structure, is also quite stable since further loss of CO occurs only if an additional 1 eV is added. Also in uracil (Mol. mass = 112.09 a.m.u.), HNCO loss is the energetically lowest lying ionic fragmentation process (AE = 10.95 eV). Further fragmentation gives the astrophysically important ion $HCNH^+$ ($m/z = 28$, AE 13.75 eV) with high intensity (see discussion on this ion below). In the non-biological bases pyrimidine and imidazole, HCN fragmentation dominates like in the case of purine, adenine and benzimidazole.

We note that quantum-chemical calculations, like those of Improta et al. (2000), on the structure and thermodynamics of fragment ions, are extremely helpful when analysing the degradation pathways.

3.2. Ionisation and dissociative ionisation of amino acids

A detailed discussion of our results for five AAs is given in Jochims et al. (2004). Major results are shown in Table 1. All the five species studied are found in meteoritic material (M. Maurette in Brack, 1998). We mention that in

biological media, AAs exist as zwitterions over a considerable range of pH values, but in the gas phase this particular form has not been observed yet so that we can assume to only study neutral monomers in our experiments. Their photoabsorption has been studied earlier (Serrano-Andrès and Fülscher, 1996 and references cited there) and shows that these molecules absorb strongly at the Lyman-α line at 10.2 eV.

For glycine (Mol. mass = 75.07 a.m.u.), the three ions $m/z = 75$, 30, 28 are present in the mass spectrum at 10 eV.With the help of PIMS measurements of fully deuterated glycine-*d*5, we could assign the $m/z = 30$ ion (AE = 9.38 ± 0.05) to be the aminomethyl radical cation, $NH_2CH_2^+$, formed by simple rupture of the C–C(OOH) bond. Formation of the CH_3NH^+ isomer is very unlikely since this species is thermodynamically less stable by 88 kJ/mol and its formation would require rearrangement, either of the parent or of the fragment ion. The third possible assignment, H_2CO^+, can also be excluded since the D_2CO^+ ion $m/z = 32$ is absent in the glycine-*d*5 mass spectrum. The glycine parent cation thus loses the COOH group at a relatively small amount of internal energy ($E_{int} = 0.36 \pm 0.07$ eV) above the first ionisation energy.

The second most intense fragment ion in the dissociative photoionisation of glycine, $m/z = 28$, is assigned to the $HCNH^+$ ion since the two other possible isomers, H_2CN^+ and CNH_2^+, are thermodynamically less stable (DeFrees and McLean, 1985). Its appearance energy is around 9 eV (the onset of this ion is very smooth so that its AE is difficult to determine) and different pathways leading to its formation have been discussed by Jochims et al. (2004).

We remark that $HCNH^+$ is observed in several galactic sources in the ISM (Schilke et al., 1991) and including the region where glycine has possibly been observed (Sgr B2). Electron capture by $HCNH^+$ is thought to be an important source of HCN (+H) and HNC (+H) in dark molecular clouds (Schilke et al., 1991; Semaniak et al., 2001). HCN and HNC are considered to be important in the synthesis of several organic molecules in the ISM. Our results suggest that $HCNH^+$ can be formed from glycine in HI regions where the upper limit of photon energies is 13.6 eV. Thus further radioastronomical searches of glycine should explore regions close to where $HCNH^+$ is observed, but where reasonable VUV shielding is present. We note that $HCNH^+$ is also an important ion in the ionosphere of Titan (Molina-Cuberos et al., 1999).

Below 13.6 eV, the principal fragment ions observed in the dissociative photoionisation of α-alanine (Mol. mass = 89.09 a.m.u.) are $m/z = 44$, 42, 28, 18. Their appearance energies and possible formation pathways have been reported by Jochims et al. (2004). Also here, earlier electron impact mass spectra of the deuterated the α-alanine-*d*3 (Junk and Svec, 1963) helped to assign the chemical structure of the ions. $HCNH^+$ is observed as an intense ion too (AE = 12.35 eV). The $m/z = 74$ ion, corresponding to the loss of the methyl group connected to the α-carbon of the parent cation, is very weak meaning that this is a minor fragmentation pathway. As in the case of glycine, the lowest lying fragmentation pathway (see Table 1) corresponds to the rupture of the C–C(OOH) bond to form $NH_2CH_3CH^+$ ($m/z = 44$).

In contrast, the most intense ion from the dissociative photoionisation of β-alanine (Mol. mass = 89.09 a.m.u.) is $m/z = 30$, corresponding to the $NH_2CH_2^+$ ion formed by bond rupture between the α- and β-carbon of the molecule leaving the CH_2COOH radical behind. $HCNH^+$ formation is less important in this molecule (AE = 14.2 ± 0.1 eV).

An interesting case is α-amino-isobutyric acid (Mol. mass = 103.12 a.m.u.). Here the appearance energy of the most intense fragment ion ($m/z = 58$) is even lower than the first IE of the molecule (see Table 1) thus implying that ion pair dissociation, forming $NH_2C(CH_3)_2^+$ and $COOH^-$, is an important contributor to the $m/z = 58$ mass peak. The second most intense fragment ion is $m/z = 42$. Its measured appearance energy (11.8 eV) suggests formation by NH_2 loss from the $NH_2C(CH_3)_2^+$ ion formed at lower energies (see the discussion in Jochims et al., 2004).

3.3. Other prebiotic molecules: formic acid, acetic acid and its isomer methylformate

Formic acid (HCOOH), acetic acid and methylformate are all observed in the ISM (Müller et al., 2005). Therefore, improvement of molecular cloud astrochemical models requires photophysical data in the VUV. These species, which we consider to be of "prebiotic" character, have been studied intensively by our group (Schwell et al., 2002; Leach et al., 2002, 2003, 2006a, b).

3.3.1. Formic acid

Firstly, we note that our high resolution (15 meV) HeI photoelectron spectra of four isotopologues of formic acid (HCOOH, DCOOH, HCOOD, DCOOD) has been recently used by Rudberg and Brinck (2004) to improve the difficult calculation of Franck-Condon factors for transitions from the ground state of the neutral molecule to the two lowest lying excited states of the formic acid cation. In this paper, we show as an extract from our results the PFS spectra recorded following VUV photoexciation of HCOOH (Figs. 5 and 6).

The dispersed fluorescence spectrum at 12 eV excitation energy (Fig. 5) is unsmoothed, but corrected for the spectral response of the detection system. At this energy, we observe two band systems, the first being the OH ($A^2\Sigma^+ \rightarrow X^2\Pi$) emissions at 308 (0–0) and 282 nm (1–0) and the second consisting of a long-vibrational progression between 330 and 480 nm (spacing of about 600 ± 40 cm^{-1}), the intensity maximum of which is at 375 nm, superimposed on a broad continuous background. Earlier work at lower energies helped to assign the emitter to be the HCOO radical (see our discussion in Schwell et al., 2002). In Fig. 6, we show the FEX spectra of the OH ($A^2\Sigma^+ \rightarrow X^2\Pi$) emission ($\lambda_{obs} = 310$ nm) and of the HCOO emission at 375 nm (Fig. 6b), from 9 to 13 eV excitation energy.

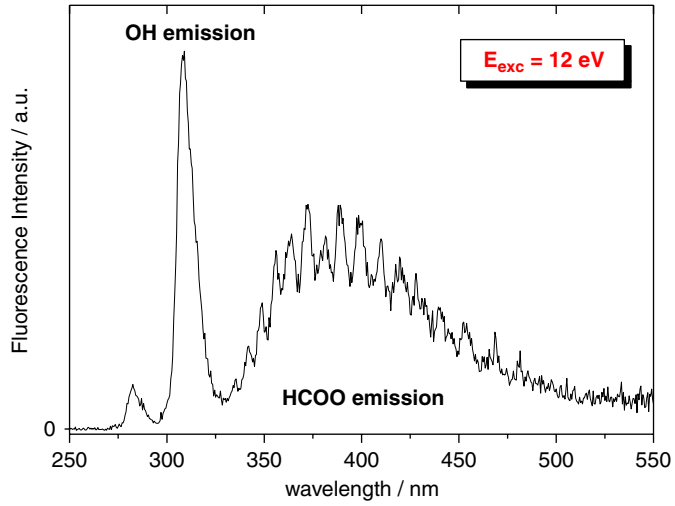

Fig. 5. Dispersed fluorescence from formic acid at 12 eV excitation energy ($\lambda_{exc} = 103$ nm).

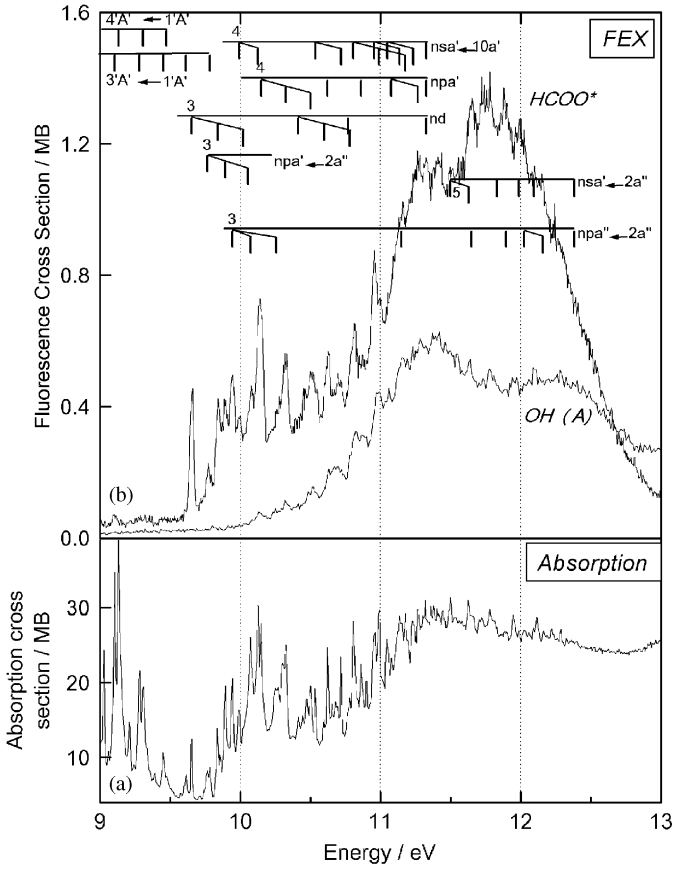

Fig. 6. (a) Photoabsorption of Formic acid. (b) Fluorescence excitation spectra (FEX) for OH and HCOO emission. Rydberg transition assignments are indicated by bars.

For comparison, we also show the photoabsorption spectrum of formic acid (Leach et al., 2002, Fig. 6a). In the FEX spectra, the weak onset of OH ($A^2\Sigma^+ \rightarrow X^2\Pi$) emission is observed at 9.15 eV (136.6 nm). From enthalpy of formation data and the OH ($A^2\Sigma^+$) T_0 value (see the NIST chemistry webbook) we can calculate the thermochemical onset for the reaction HCOOH → HCO + OH ($A^2\Sigma^+$) to be 8.85 eV.This is about 300 meV below our measured onset energy of the OH (A) emission. This difference indicates the existence of a potential barrier between the HCOOH excited state and the dissociation surface leading to the OH (A) fragment. This is consistent with the slow rise of the OH emission yield in the first electron volt beyond the onset, which is typical for photochemical dissociations involving potential barriers. Also the HCOO FEX spectrum increases with increasing photon energy below the first IE. Furthermore, it appears that most of the features observed in the OH (A) FEX spectrum are also observed in the HCOO FEX spectrum but with different relative intensities. This is particularly evident, for example, in the energy region between 10 and 11 eV (see Fig. 6b). It indicates that the corresponding HCOOH excited states can fragment into each of the two dissociation channels. However, the branching ratio of the two dissociation reactions HCOOH → HCO + OH (A) and HCOOH → HCOO ($^2B_1$) + H varies considerably as a function of excitation energy as is evident from Fig. 6.

3.3.2. *Acetic acid and its isomer methylformate*

Two papers on the VUV photophysics of acetic acid have been published very recently: The photoabsorption of this molecule has been analysed in detail by Leach et al. (2006a). PIMS and PFS experiments were also performed for this important species (Leach et al., 2006b). We further mention the pioneering work of Suto et al. (1988) who measured absorption cross sections and fluorescence quantum yields from photodissociative excitation of these molecules below 11.2 eV. The acetic acid absorption spectrum (Fig. 7a, bandwidth 0.9 Å) shows valence transitions as well as Rydberg transitions converging to the ground state of the CH_3COOH^+ ion ($IE_{CH_3COOH} = 10.58 \pm 0.02$ eV, Leach et al., 2006b). Band attributions will not be discussed in this paper, they are given in Leach et al. (2006a). In Fig. 7b we also include the absorption spectrum of the isomer methylformate (bandwidth 0.9 Å). Also in this molecule, Rydberg transitions converging to the first ionisation energy, at 10.835 eV (Waterstradt et al., 1994), are observed. Several broad features are observed between 11 and 18 eV, like in the case of acetic acid. A detailed analysis of the methylformate absorption spectrum will be given in a forthcoming publication.

To our knowledge, the absolute absorption spectra of both compounds were not known above 11.2 eV.The two spectra presented in Fig. 7 are qualitatively similar in that the absolute cross sections are continuously increasing between 6 and 17 eV, starting from 0 Mb reaching a plateau value of about 70 Mb at 17 eV (1 Mb = 10^{-18} cm^2). We note that below 6 eV the cross section is not zero for both molecules: a very weak band, extending from about 200 nm (6.2 eV) to about 240 nm (5.2 eV) has been observed by Suto et al. (1988), with cross sections below 0.3 Mb. These bands correspond to the lowest lying singlet–singlet transitions of the two molecules ($\pi^* \leftarrow n_O$). In our experiment, the grating transmittance of the primary

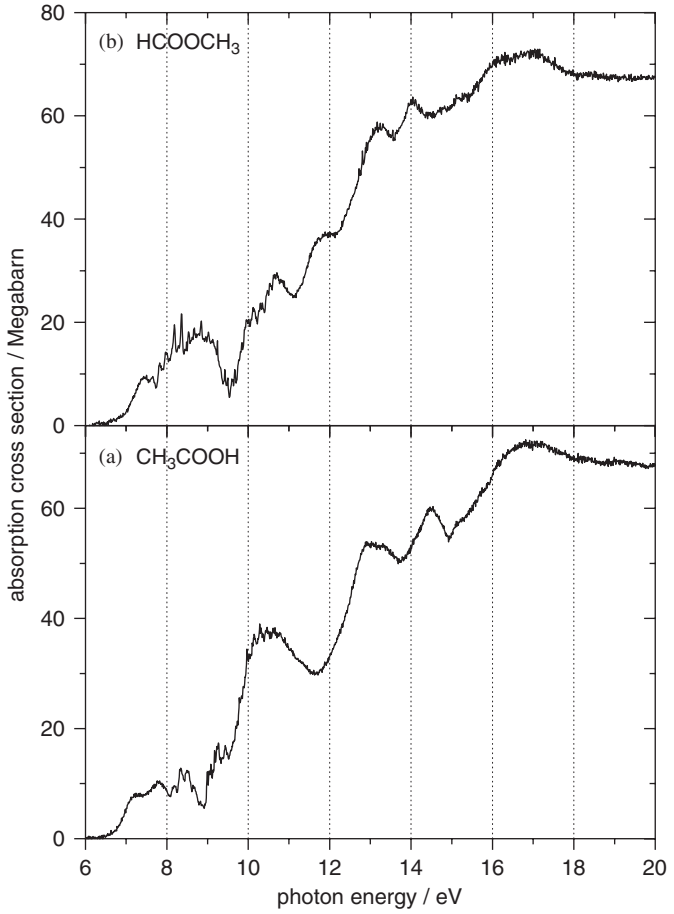

Fig. 7. Comparison of VUV photoabsorption spectra of acetic acid and methyl formate, between 6 and 22 eV (bandwidth 0.9 Å).

monochromator was not sufficient below 6 eV in order to observe such weak bands.

4. Conclusion and astrophysical implications

In this paper we reviewed results obtained recently by our group, on the photochemistry of small biomolecules and some prebotic species in the VUV spectral region (6–20 eV). The results are important in an exobiological context, concerning the prediction of the photostability of these molecules in VUV radiation fields.

Extensive PIMS measurements have been performed on nearly all of the molecules studied. The results enabled us to give new thermochemical values for many cations, parent and fragments. The parent cations of NABs are found to be stable for fairly large internal energies E_{int} above the ionisation limit (for example adenine: 8.2–11.56 eV, 140–107 nm, $E_{int} = 3.36$ eV). Since our appearance energy measurements correspond to a photodissociation rate of about $k_{diss} = 10^4\,s^{-1}$ at the measured ion onset (Jochims et al., 1994), we can suppose that in the energy domain from the first IE up to the first fragment AE the NAB cations would preferably relax via IVR (internal vibrational rotational redistribution) and related to infrared emission in the virtually collisionless conditions of the ISM, as discussed by Jochims et al. (1994). However, this hypothesis has to be confirmed by measurements of the IR emission rate of these molecules. We hypothesise further that the relative stability of NAB cations can be associated with their aromatic ring system, capable of stabilising a positive charge.

The VUV fragmentation of NABs and AAs is quite complex and has been analysed in detail by Jochims et al. (2004, 2005). In the present paper we discussed the most important fragmentation reactions.

The dominant ionic fragmentation channel of the NABs in the $E < 13.6$ eV energy regime is loss of HCN which is observed for adenine, purine, benzimidazole, pyrimidine, and imidazole. In thymine and uracil, however, HNCO loss is the lowest lying fragmentation channel. We note that HCN and HNCO are both observed in cometary atmospheres (Cottin et al., 1999). HCN (but not HNCO) is observed in the atmosphere of Titan and vertical profiles have been retrieved recently by the UVIS spectrometer on board the Cassini spacecraft (Shemansky et al., 2005). We speculate that these molecules may originate, in part, from NABs or other aromatic nitrogen heterocycles, photodegraded in the VUV. Solar system searches for NABs should therefore be focused on objects and regions where their fragments HCN and HNCO are observed.

The radical CN is another important species observed in cometary atmospheres (see Fray et al., 2005 and references cited therein) and in the ISM (Müller et al., 2005). This radical is apparently not produced in the VUV photodissociation of gaseous NABs at energies below 20 eV, since the counter-ion $(M–CN)^+$ is not observed and none of the postulated fragmentation pathways in the VUV involve the loss of neutral CN (Jochims et al., 2005). In cometary atmospheres CN originates mostly from the photodissociation of HCN but also other sources, like solid HCN polymers, have been considered to contribute to the observed CN production rate (Fray et al., 2005).

AA parent cations fragment at only small internal energies above the ionisation limit (Jochims et al., 2004) and their stability against VUV radiation is therefore very much reduced as compared to NABs. The lowest lying fragmentation reaction of the AAs studied is rupture of the C–C(OOH) bond to give the $(M–COOH)^+$ ion and neutral COOH or CO_2 and H. This result is qualitatively consistent with the experiments at lower energies performed by Ehrenfreund et al. (2001) who observed the CO_2 IR absorption bands upon irradiation of AAs. The additional H-loss of the primary photofragment COOH in the matrix experiments remains to be explained since this reaction is endothermic (in contrast to the reaction $HCOO \rightarrow CO_2 + H$ which is exothermic). Sometimes COOH is also referred to as "HOCO". This species should not to be confused with its isomer HCOO which is a principal fragment in the VUV degradation of formic acid (see above). We note that the $HOCO^+$ ion is also observed in the ISM (Müller et al., 2005).

The astrophysically important $HCNH^+$ ion is observed in the dissociative photoionisation of glycine (AE = 13.0 ± 0.1 eV), α-alanine (12.35 eV), β-alanine (AE = 14.2 ± 0.1 eV), α-amino-isobutyric acid and α-valine (AE determination not possible for the latter two AAs). Searches for glycine or other AAs should thus be focused on regions where this ion is present and at the same time shielding by solid material can be expected.

Our study of the prebiotic species HCOOH, CH_3COOH, $HCOOCH_3$, all observed in the ISM, revealed their principal fragmentation pathways in the VUV. Their photoabsorption cross sections have also been measured, from 6 to 22 eV (bandwith 0.9 Å). Absorption spectra of these species above 11.2 eV were not known before. When HCOOH is excited with photon energies that correspond to astrophysical HI regions ($E_{photon} < 13.6$ eV) we detect OH ($A^2\Sigma^+ \rightarrow X^2\Pi$) emission and HCOO* emission in the UV/Vis spectral region, related to the photoreactions $HCOOH \rightarrow OH\ (A^2\Sigma^+) + HCO$ and $HCOOH \rightarrow H + HCOO^*$ which hence must be considered as important photoreactions in the VUV for $E > 9.5$ eV. Although in our experiments we cannot observe non-fluorescent fragments it is reasonable to assume that the same photoreactions yielding the fragments in their respective ground states are important, also below 9.5 eV. The yields of these processes however remain to be quantified. Since HCOO is thermodynamically unstable with respect to CO_2 and H, the photodissociation processes $HCOOH \rightarrow OH + HCO$ and $HCOOH \rightarrow 2H + CO_2$ constitute the main fragmentation pathways of formic acid below 13.6 eV.

In the VUV excited photodissociation of Acetic acid we detect OH ($A^2\Sigma^+ \rightarrow X^2\Pi$), CH ($A^2\Delta \rightarrow X^2\Pi$), CH ($B^2\Sigma^- \rightarrow X^2\Pi$) and H-Balmer transition features in the UV/Vis spectral domain. The related fragmentation processes are analysed in detail by Leach et al. (2006b). No other emissions were observed from VUV excited acetic acid, in particular none from the HCOO radical. This confirms, from the chemical structure of these molecules, the assignment of HCOO (and not COOH) being formed as primary fragment in the formic acid photodissociation.

Considering the importance of ionic dissociation channels in the photochemistry of the biomolecules studied measurements of their photoionisation quantum yields (γ_{ion}) have to be undertaken as a function of photon energy, in order to measure the branching ratio of ionic channels as compared to neutral photodissociation and internal conversion (IVR) to the electronic ground state. Earlier γ_{ion}-measurements of polycyclic aromatic hydrocarbons (PAHs, Jochims et al., 1996) showed that this quantity can reach up to 50%at internal energies E_{int} of about 3 eV above the first ionisation energy. The region of competitive non-ionic decay processes ($\gamma_{ion} < 1$) extends further up to about IE + 9.2 eV for these molecules. We speculate that especially the chemically related NABs could show similar behaviour thus making ionisation an important pathway to stabilise these molecules in VUV radiation fields. Their cations could later recombine with low energy electrons to restore the neutral molecules.

γ_{ion} has also been measured for formic acid, as a function of photon energy (Schwell et al., 2002). It steadily increases, from the first ionisation energy at 11.33 eV (NIST evaluated value), reaching a plateau value of γ_{ion} = unity at 18 ± 0.1 eV. The region of competitive non-ionic decay processes (IE + 6.67 ± 0.1 eV) is thus smaller than in PAHs. The γ_{ion} curve of HCOOH shows steps whenever an ionic state becomes accessible.

Acknowledgements

The authors wish to thank Jean-Louis Chotin for valuable assistance during beam time periods. H.B. thanks the Fonds der Chemischen Industrie. M.S. wishes to thank François Raulin for the loan of several exobiology text books. We are grateful for support from the European Commission programme "Access to Research Infrastructures" for providing access to the Berlin BESSY synchrotron facility under contract FMRX-CT-O126. Welcome support from the CNRS Groupe de Recherche "GDR Exobiologie" (GDR 1877) and from INSU is gratefully acknowledged. We finally thank Gerd Reichardt and Andreas Balzer for support during current runs at BESSY.

References

Arakawa, E.T., Emerson, L.C., Juan, S.I., Ashley, J.C., Williams, M.W., 1986. The optical properties of Adenine from 1.8 to 80 eV. Photochem. Photobiol. 44, 349–353.

Basile, B., Lazcano, Oro, J., 1984. Prebiotic syntheses of purines and pyrimidines. Adv. Space Res. 4, 125–131.

Berry, R.S., Leach, S., 1981. Elementary attachment and detachment processes II. Adv. Electron. Electron Phys. 57, 1.

Brack, A. (Ed.), 1998. The Molecular Origins of Life. Oxford University Press, Oxford.

Broo, A., 1998. A theoretical investigation of the physical reason for very different luminescence properties of the two isomers adenine and 2-aminopurine. J. Phys. Chem. 102, 526.

Callis, P.R., 1983. Electronic states and luminescence of nucleic acid systems. Annu. Rev. Phys. Chem. 34, 329.

Chase Jr., M.W., 1998. NIST-JANAF themochemical tables, fourth ed. J. Phys. Chem. Ref. Data Monogr. 9, 1-1951, accessible through http://webbook.nist.gov.

Chela-Flores, J., Owen, T., Raulin, F. (Eds.), 2001. First Steps in the Origin of Life in the Universe. Kluwer Academic Publishers, Dordrecht.

Chyba, C., Sagan, C., 1992. Endogenous production, exogenous delivery and impact-shock synthesis of organic molecules: an inventory for the origins of life. Nature 355, 125.

Cottin, H., Gazeau, M.C., Raulin, F., 1999. Cometary organic chemistry: a review from observations, numerical and experimental simulations. Planet. Space Sci. 47, 1141–1162.

Cronin, J.R., 1976a. Acid-labile amino acid precursors in the Murchison meteorite 1: chromatographic fractionation. Origins Life 7, 337–342.

Cronin, J.R., 1976b. Acid-labile amino acid precursors in the Murchison meteorite 2: a search for peptides and amino acyl amides. Origins Life 7, 343–348.

Cronin, J.R., Pizzarello, S., 1983. Amino acids in meteorites. Adv. Space Res. 3, 5–18.

DeFrees, D.J., McLean, A.D., 1985. Does carbon-protonated Hydrogen cyanide, H_2CN^+, exist ? J. Am. Chem. Soc. 107, 4350–4351.

Ehrenfreund, P., Bernstein, M.P., Dworkin, J.P., Sandford, S.A., Allamandola, L.J., 2001. The photostability of amino acids in space. Astrophys. J. 550, L95–L99.

Fray, N., Benilan, Y., Cottin, H., Gazeau, M.-C., Crovisier, J., 2005. The origin of the CN radical in comets: A review from observations and models. Planet. Space Sci. 53, 1243–1262.

Hayatsu, R., Studier, M.H., Moore, L.P., Anders, E., 1975. Purines and triazines in the murchison meteorite. Geochim. Cosmochim. Acta 39, 471–488.

Hua, L.-L., Kobayashi, K., Ochiai, E.-I., Gerke, C.W., Gerhardt, K.O., Ponnamperuma, C., 1986. Identification and quantification of nucleic acid cases in carbonaceous chondrites. Origins Life 16, 226–227.

Improta, R., Scalmani, G., Barone, V., 2000. Radical cations of DNA bases: some insights on structure and fragmentation patterns by density functional methods. Int. J. Mass Spectrom. 201, 321–336.

Irvine, W.M., Elldér, J., Hjalmarson, A., Kollberg, E., Rydbeck, O.E.H., Sorensen, G.O., Bak, B., Svanholt, H., 1981. Searches for interstellar imidazole and cyanoform. Astron. Astrophys. 97, 192–194.

Isaacson, M., 1972. Interaction of 25 keV electrons with the nucleic acid bases adenine, thymine, and uracil. i. outer shell excitation. J. Chem. Phys. 56, 1803–1812.

Jochims, H.-W., Rühl, E., Baumgärtel, H., Tobita, S., Leach, S., 1994. Size effects on dissociation rates of polycylic aromatic hydrocarbons: laboratory studies and astrophysical implications. Astrophys. J. 420, 307–317.

Jochims, H.-W., Baumgärtel, H., Leach, S., 1996. Photoionsiation quantum yields of polycyclic aromatic hydrocarbons. Astron. Astrophys. 314, 1003–1009.

Jochims, H.-W., Schwell, M., Chotin, J.-L., Clémino, M., Dulieu, F., Baumgärtel, H., Leach, S., 2004. Photoion mass spectrometry of five amino acids in the 6–22 eV photon energy range. Chem. Phys. 298, 279–297.

Jochims, H.-W., Schwell, M., Baumgärtel, H., Leach, S., 2005. Photoion mass spectrometry of adenine, thymine and uracil in the 6–22 eV energy range. Chem. Phys. 314, 263–282.

Junk, G., Svec, H., 1963. The mass spectra of the α-amino acids. J. Am. Chem. Soc. 85, 839–845.

Kissel, J., Krueger, F.R., 1987. The organic component in dust from comet Halley as measured by the PUMA mass spectrometer on board Vega 1. Nature 326, 755.

Kuan, Y.-J., Yan, C.-H., Charnley, S.B., Huang, H.C., Tseng, W.-L., Kisiel, Z., 2003a. Interstellar glycine. Astrophys. J. 593, 848–867.

Kuan, Y.-J., Yan, C.-H., Charnley, S.B., Kisiel, Z., Ehrenfreund, P., Huang, H.-C., 2003b. A search for interstellar pyrimidine. Monthly Notices Roy. Astron. Soc. 345, 650.

Lavrentiev, G.A., Strigunkova, T.F., Egorov, I.A., 1984. A biological synthesis of amino acids, purines and pyrimidines under conditions simulating the volcanic ash-gas cloud. Origins Life 14, 205–212.

Leach, S., Schwell, M., Dulieu, F., Chotin, J.-L., Jochims, H.W., Baumgärtel, H., 2002. Photophysical studies of formic acid in the VUV. Absorption spectrum in the 6–22 eV region. Phys. Chem. Chem. Phys. 4, 5025–5039.

Leach, S., Schwell, M., Talbi, D., Berthier, G., Hottmann, K., Jochims, H.W., Baumgärtel, H., 2003. He I photoelectron spectroscopy of four isotopologues of formic acid: HCOOH, HCOOD, DCOOH and DCOOD. Chem. Phys. 286, 15–43.

Leach, S., Schwell, M., Un, S., Jochims, H.-W., Baumgärtel, H., 2006a. VUV absorption spectrum of acetic acid between 6 and 22 eV. Chem. Phys. 321, 159–170.

Leach, S., Schwell, M., Jochims, H.-W., Baumgärtel, H., 2006b. VUV photophysics of acetic acid: fragmentation, fluorescence and ionisation in the 6–23 eV region. Chem. Phys. 321, 171–182.

Lührs, D.C., Viallon, J., Fischer, I., 2001. Excited state spectroscopy of isolated adenine and 9-methyl adenine. Phys. Chem. Chem. Phys. 3, 1827–1831.

Maurel, M.C., Décout, 1999. Origins of life: molecular foundations and new approaches. Tetrahedron 55, 3141–3182.

Minard, R.D., Hatcher, P.G., Gourley, R.C., Matthews, C.N., 1998. Structural investigation of hydrogen cyanide polymers: new insights using TMAH thermochemolysis/GC-MS. Origins Life Evol. Biosphere 28, 461–473.

Molina-Cuberos, G.J., Lopez-Moreno, J.J., Rodrigo, R., Lara, L.M., O'Brien, K., 1999. Ionisation by cosmic rays of the atmosphere of Titan. Planet. Space Sci. 47, 1347–1354.

Müller, H.S.P., Schlöder, F., Stutzki, J., Winnewisser, G., 2005. The Cologne database for molecular spectroscopy, CDMS: a useful tool for astronomers and spectroscopists. J. Mol. Structure 742, 215–227.

Muñoz Caro, G.M., Meierhenrich, U.J., Schutte, W.A., Barbier, B., Arcones Segovia, A., Rosenbauer, H., Thiemann, W., Brack, A., Greenberg, J.M., 2002. Amino acids from ultraviolet irradiation of interstellar ice analogues. Nature 416, 403.

Nir, E., Kleinermanns, K., Grace, L., de Vries, M.S., 2001. On the photochemistry of purine nucleobases. J. Phys. Chem. A 105, 5106–5110.

Peeters, Z., Botta, O., Charnley, S.B., Ruiterkamp, R., Ehrenfreund, P., 2003. The astrobiology of nucleobases. Astrophys. J. 593, L129–L132.

Plützer, C., Kleinermanns, K., 2002. Tautomers and electronic states of jet-cooled adenine investigated by double resonance spectroscopy. Phys. Chem. Chem. Phys. 4, 4877–4882.

Plützer, C., Nir, E., de Vries, M.S., Kleinermanns, K., 2001. IR-UV double resonance spectroscopy of the nucleobase adenine. Phys. Chem. Chem. Phys. 3, 5466–5469.

Robin, M.B., 1974. Higher Excited States of Polyatomic Molecules. Academic Press, New York.

Rudberg, E., Brinck, T., 2004. Computation of Franck-Condon factors for many-atom systems: simulated photoelectron spectra of formic acid isotopologues. Chem. Phys. 302, 217–226.

Samson, J.A.R., Ederer, D.L. (Eds.), 2000. Vacuum Ultraviolet Spectroscopy. Academic Press, London.

Schilke, P., Walmsley, C.M., Millar, T.J., Henkel, C., 1991. Protonated HCN in molecular clouds. Astron. Astrophys. 247, 487–496.

Schwell, M., Dulieu, F., Gée, G., Jochims, H.-W., Chotin, J.-L., Baumgärtel, H., Leach, S., 2000. Photionisation mass spectrometry of six isomers of C_7H_8 in the 7–22 photon energy range. Chem. Phys. 260, 261.

Schwell, M., Dulieu, F., Jochims, H.-W., Fillion, J.-H., Lemaire, J.-L., Baumgärtel, H., Leach, S., 2002. Photophysical studies of formic acid in the vacuum-UV: fragmentation, fluorescence and ionisation. J. Phys. Chem. A 106, 10908–10918.

Schwell, M., Jochims, H.-W., Baumgärtel, H., Leach, S., 2006. Photoion mass spectrometry of purine, pyrimidine, benzimidazole and imidazole in the 7–15 eV energy range. (Manuscript in preparation).

Semaniak, J., Minaev, B.F., Derkatch, A.M., Hellberg, F., Neau, A., Rosén, S., Thomas, R., Larsson, M., Danared, H., Paál, A., Af Ugglas, M., 2001. Dissociative recombination of $HCNH^+$: absolute cross-sections and branching ratios. Astrophys. J. Suppl. Ser. 135, 275–283.

Serrano-Andrès, L., Fülscher, M.P., 1996. Theoretical study of the electronic spectroscopy of peptides. 2. glycine and N-acetylglycine. J. Am. Chem. Soc. 118, 12200–12206.

Shemansky, D.E., Stewart, A.I.F., West, R.A., Esposito, L.W., Hallett, J.T., Liu, X., 2005. The Cassini UVIS stellar probe of the titan atmosphere. Science 308, 978–982.

Sowerby, S.J., Heckel, W.M., 1998. The role of self-assembled monolayers of the purine and pyrimidine bases in the emergence of life. Origins Life Evol. Biosphere 28, 283–310.

Sowerby, S.J., Petersen, G.B., Holm, N.G., 2001. Primordial coding of amino acids by adsorbed purine bases. Origins Life Evol. Biosphere 32, 35–46.

Stocks, P.G., Schwartz, A.W., 1981. Nitrogen-heterocyclic compounds in meteorites: significance and mechanisms of formation. Geochim. Cosmochim. Acta 45, 563–569.

Suto, M., Wang, X., Lee, L.C., 1988. Fluorescence yields form photodissociative excitation of HCOOH, $HCOOCH_3$, CH_3COOH in the vacuum-ultraviolet region. J. Phys. Chem. 92, 3764–3768.

Waterstradt, E., Jung, R., Belling, T., Muller-Dethlefs, K., 1994. Zero kinetic energy (ZEKE) photoelectron spectrum and coincident mass spectra of methylformate. Ber. Bunsenges. Phys. Chem. 98, 176.